NEUROSCIENCE

PRMT8 as a phospholipase regulates Purkinje cell dendritic arborization and motor coordination

10.1126/sciadv.1500615

Jun-Dal Kim,[1] Kyung-Eui Park,[2] Junji Ishida,[1] Koichiro Kako,[2] Juri Hamada,[1] Shuichi Kani,[3] Miki Takeuchi,[4,5] Kana Namiki,[6] Hajime Fukui,[7] Shigetomo Fukuhara,[7] Masahiko Hibi,[3,4] Makoto Kobayashi,[5] Yasunori Kanaho,[8] Yoshitoshi Kasuya,[6] Naoki Mochizuki,[7,9] Akiyoshi Fukamizu[1,2,10]*

The development of vertebrate neurons requires a change in membrane phosphatidylcholine (PC) metabolism. Although PC hydrolysis is essential for enhanced axonal outgrowth mediated by phospholipase D (PLD), less is known about the determinants of PC metabolism on dendritic arborization. We show that protein arginine methyltransferase 8 (PRMT8) acts as a phospholipase that directly hydrolyzes PC, generating choline and phosphatidic acid. We found that PRMT8 knockout mice (*prmt8*$^{-/-}$) displayed abnormal motor behaviors, including hindlimb clasping and hyperactivity. Moreover, *prmt8*$^{-/-}$ mice and TALEN-induced zebrafish *prmt8* mutants and morphants showed abnormal phenotypes, including the development of dendritic trees in Purkinje cells and altered cerebellar structure. Choline and acetylcholine levels were significantly decreased, whereas PC levels were increased, in the cerebellum of *prmt8*$^{-/-}$ mice. Our findings suggest that PRMT8 acts both as an arginine methyltransferase and as a PC-hydrolyzing PLD that is essential for proper neurological functions.

INTRODUCTION

In vertebrates, the cerebellum plays a crucial role in learning, balance, behavior, and attention (*1*, *2*). Arborization in Purkinje cells is an important step in the formation of extensive dendritic trees, which are essential for cerebellum functions (*3*). The development of neurons is characterized by morphogenetic processes such as neurite outgrowth, elongation, and branching (*4*) which are critically dependent on the hydrolysis and biosynthesis of phosphatidylcholine (PC) (*5*–*7*). Despite the essential roles of PC metabolism in axonal outgrowth and elongation (*8*, *9*), the type of enzymes involved in dendritic arborization remains an open question.

The protein arginine methyltransferase 8 (PRMT8) is a brain-specific member of the PRMT family and is anchored to the phospholipid bilayer on the plasma membrane through myristoylation (*10*). Recombinant glutathione *S*-transferase– or His-tagged PRMT8 proteins expressed in *Escherichia coli* cells catalyze the methylation of arginine residues in vitro (*10*–*12*) and are automethylated in the N-terminal region, which negatively regulates its enzymatic activity (*13*, *14*). A recent study reported that PRMT8 regulates the retinoic acid–dependent differentiation of embryonic stem cells (*15*) and may play important roles in neural development during early zebrafish embryogenesis (*16*). In addition, PRMT8 is expressed mainly in dendrites of mouse cerebellar Purkinje cells during maturation (*17*). However, the role of PRMT8 has not been characterized because no endogenous plasma membrane substrate(s) has been found in mammals to date. Here, we propose that PRMT8 is important for the dendritic morphology of Purkinje cells and, as a phospholipase, maintains coordinating behaviors, generating choline and phosphatidic acid (PA) directly from PC.

RESULTS AND DISCUSSION

To identify an in vivo role of PRMT8, we generated homozygous PRMT8 knockout mice (*prmt8*$^{-/-}$) lacking exon 5 of the mouse gene (accession number NM_201371) (Fig. 1A), which encodes a Rossmann fold domain (*18*) homologous to amino acids 161 to 208 of human PRMT8 (accession number NP_062828). The deletion was confirmed by polymerase chain reaction (PCR) analysis (Fig. 1B).

PRMT8 is expressed in the Purkinje cells of mouse (*17*) and zebrafish cerebellum (fig. S1A). Quantitative real-time PCR (qPCR) indicated that the expression of *prmt8* mRNA in the cerebellum was decreased by 45% in heterozygous knockout *prmt8* mice (*prmt8*$^{+/-}$) and by >95% in *prmt8*$^{-/-}$ mice compared to wild-type mice (*prmt8*$^{+/+}$) (Fig. 1C). Immunofluorescence analysis with an anti-calbindin antibody showed stunted growth of the dendritic trees in Purkinje cells of *prmt8*$^{-/-}$ mice (Fig. 1D). Furthermore, both the *prmt8b* (an ortholog of human *prmt8*) knockout zebrafish (*prmt8b*$^{ncv102/ncv102}$) and the *prmt8b* morphants also showed morphological changes at the midbrain/hindbrain boundary and reduced dendritic arborization of Purkinje cells (fig. S1, B to G).

Purkinje cells have highly branched dendritic trees (*3*, *19*), which play an important role in cerebellar motor performance (*20*). Although *prmt8*$^{-/-}$ mice grew and reproduced normally (data not shown), at 10 to 14 weeks of age, they clasped their hindlimbs when lifted by the tail (Fig. 1E) and displayed a hyperactive phenotype when exposed to novel environments, such as a new cage (movie S1). Moreover, *prmt8*$^{-/-}$ mice displayed gait abnormalities in footprint analysis:

[1]Life Science Center, Tsukuba Advanced Research Alliance (TARA), University of Tsukuba, 1-1-1 Tennoudai, Tsukuba 305-8577, Japan. [2]Graduate School of Life and Environmental Sciences, University of Tsukuba, 1-1-1 Tennoudai, Tsukuba 305-8572, Japan. [3]Laboratory for Vertebrate Axis Formation, RIKEN Center for Developmental Biology, Kobe, Hyogo 650-0047, Japan. [4]Laboratory of Organogenesis and Organ Function, Bioscience and Biotechnology Center, Nagoya University, Nagoya, Aichi 464-8601, Japan. [5]Department of Molecular and Developmental Biology, Faculty of Medicine, University of Tsukuba, 1-1-1 Tennoudai, Tsukuba 305-8575, Japan. [6]Department of Biochemistry and Molecular Pharmacology, Graduate School of Medicine, Chiba University, 1-8-1 Inohana, Chiba 260-8670, Japan. [7]Department of Cell Biology, National Cerebral and Cardiovascular Center Research Institute, Fujishirodai 5-7-1, Suita, Osaka 565-8565, Japan. [8]Department of Physiological Chemistry, Faculty of Medicine and Graduate School of Comprehensive Human Sciences, University of Tsukuba, 1-1-1 Tennoudai, Tsukuba 305-8575, Japan. [9]AMED-CREST, National Cerebral and Cardiovascular Center Research Institute, Fujishirodai 5-7-1, Suita, Osaka 565-8565, Japan. [10]International Institute for Integrative Sleep Medicine (WPI-IIIS), University of Tsukuba, 1-1-1 Tennoudai, Tsukuba 305-8575, Japan.
*Corresponding author. E-mail: akif@tara.tsukuba.ac.jp

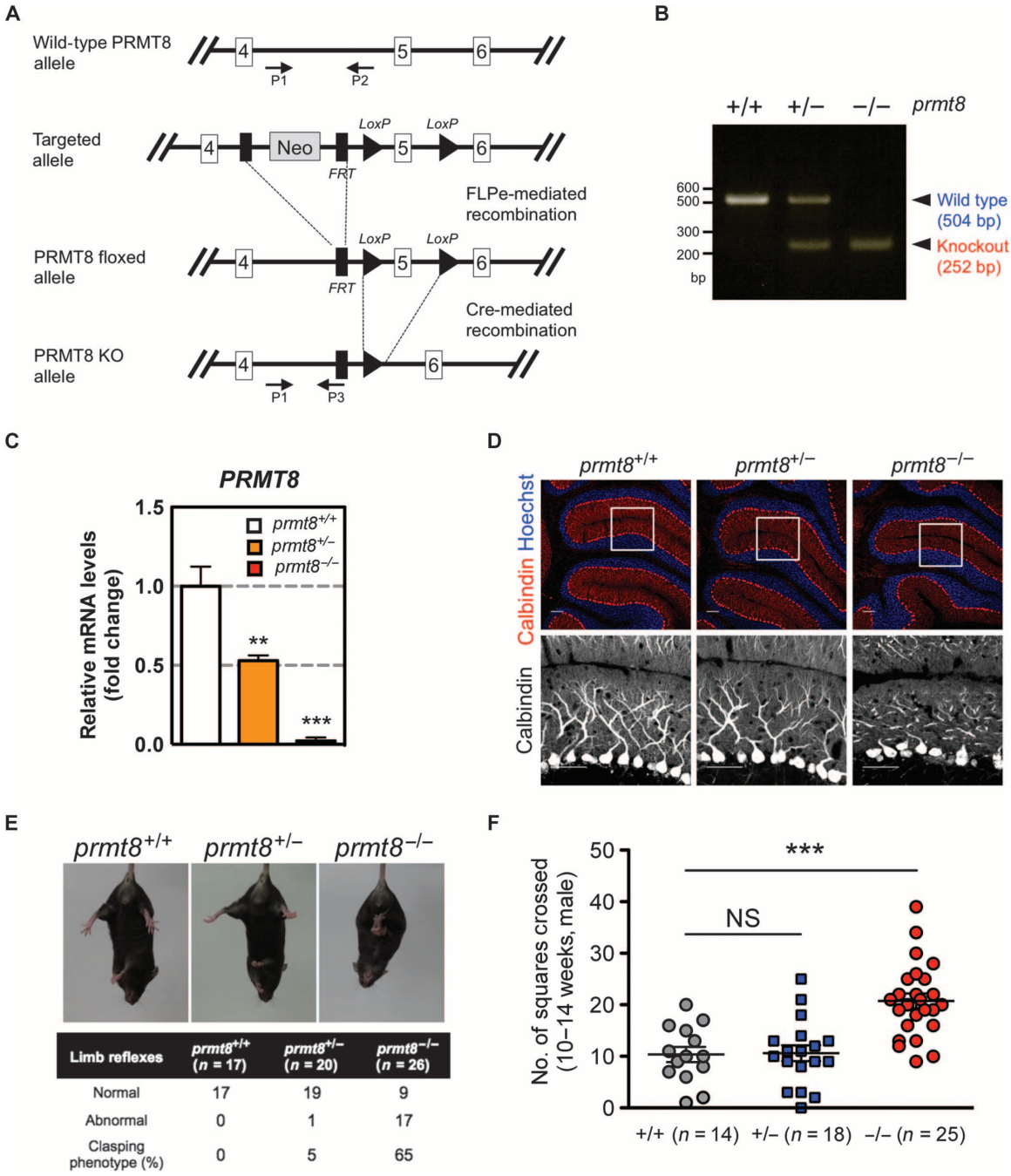

Limb reflexes	$prmt8^{+/+}$ (n = 17)	$prmt8^{+/-}$ (n = 20)	$prmt8^{-/-}$ (n = 26)
Normal	17	19	9
Abnormal	0	1	17
Clasping phenotype (%)	0	5	65

Fig. 1. PRMT8 knockout mice display abnormal Purkinje cell dendrites and aberrant behavior. (**A**) Gene targeting strategy for the *prmt8* locus: schematic representation of the $prmt8^{+/+}$ [wild-type (WT)], $prmt8^{flox}$ (floxed), and $prmt8^{-/-}$ (knockout) alleles. Arrows indicate the positions of the P1, P2, and P3 genotyping primers. (**B**) Allele-specific PCR analysis using tail genomic DNA. Products of 504 and 252 base pairs (bp) were generated from $prmt8^{+/+}$ and $prmt8^{-/-}$ mice, respectively. (**C**) *prmt8* mRNA levels in 12-week-old mice were examined in total cerebellar RNA by qPCR. Results are shown as fold change of *prmt8* mRNA expression relative to the mean WT value. Data were obtained using the $\Delta\Delta C_t$ method with normalization to the reference glyceraldehyde-3-phosphate dehydrogenase (*GAPDH*) mRNA (mean ± SEM, $n = 4$ per genotype; $^{**}P < 0.05$, $^{***}P < 0.0001$). (**D**) Top: Representative confocal images of cerebellar sections from 12- to 14-week-old animals (genotyped as indicated) stained for immunofluorescence detection of calbindin (red) to indicate Purkinje cells and Hoechst 33258 (blue) to label DNA (scale bars, 20 μm). Bottom: Enlarged images of the boxed areas with the Purkinje cell layer (scale bars, 20 μm). (**E**) Limb-clasping reflex in 10- to 14-week-old mice suspended by the tail as monitored by video recording. The percentage indicates the limb-clasping reflex of mice (genotyped as indicated). (**F**) Locomotor activity of $prmt8^{-/-}$ mice. The total number of squares crossed by the insect during 30 s is indicated. Data are shown as means ± SEM; $^{***}P < 0.0001$ or NS (not significant) as compared to WT animals.

the sway length and the stance length were significantly shorter than those of the wild-type mice (fig. S2). Thus, we focused on the motor function of the cerebellum because the *prmt8*$^{-/-}$ mouse phenotype strongly pointed to a cerebellar origin. Open-field behavioral assays are commonly used to test the locomotor activity of rodents (*21*, *22*). We scored the number of squares crossed for 30 s. *prmt8*$^{-/-}$ mice exhibited a twofold increase in spontaneous behavioral hyperactivity as compared to *prmt8*$^{+/-}$ and *prmt8*$^{+/+}$ mice (Fig. 1F). These results suggest that PRMT8 is involved in the cerebellar-dependent behavioral systems, including motor coordination and attention.

Acetylcholine is an important neurotransmitter that plays a key role in the coordination of attention behavior (*23*–*25*). A number of studies have demonstrated that reduced amounts of acetylcholine lead to hyperactivity in animals (*26*–*28*). We used matrix-assisted laser desorption/ionization–quadrupole ion trap time of flight mass spectrometry (MALDI-QIT-TOF/MS) to measure acetylcholine levels and compared the peak intensity and peak area of the signal at mass-to-charge ratio (*m*/*z*) 146 $[M]^+$ among *prmt8*$^{-/-}$ mice and the *prmt8*$^{+/-}$ and *prmt8*$^{+/+}$ control groups. The results showed that acetylcholine levels were significantly decreased in the *prmt8*$^{-/-}$ cerebellum (Fig. 2, A and B). Acetylcholine is synthesized from choline (a product of PC-derived hydrolysis) by choline acetyltransferase (ChAT) in the brain (*29*–*31*). Therefore, we also used MS to measure choline levels and found that the signal at *m*/*z* 104 $[M]^+$ was significantly reduced in the *prmt8*$^{-/-}$ and *prmt8*$^{+/-}$ cerebella as compared to the *prmt8*$^{+/+}$ cerebellum (Fig. 2, C and D). By contrast, dipalmitoylphosphatidylcholine (DPPC; *m*/*z* 757 $[M + Na]^+$), a major PC in the brain, was markedly increased in the *prmt8*$^{-/-}$ cerebellum as compared to the *prmt8*$^{+/-}$ and *prmt8*$^{+/+}$ cerebella (Fig. 2, E and F). Given the reduced levels of acetylcholine and choline accompanied by increased PC levels, these data suggested that PC was not efficiently hydrolyzed in *prmt8*$^{-/-}$ mice.

To understand how DPPC levels were increased in *prmt8*$^{-/-}$ mice, we examined the expression of enzymes involved in the PC metabolic pathway in the cerebellum, including ChAT, phospholipase D1 (PLD1), and PLD2. The latter two enzymes are major factors in PC hydrolysis, generating choline and PA (*32*), which also serve to regulate neurite outgrowth in mammals (*8*). We measured the mRNA levels of these enzymes by qPCR and showed that the expression of the genes for ChAT and the two main PLDs (PLD1 and PLD2) was not statistically significant among the three genotypes (*prmt8*$^{-/-}$, *prmt8*$^{+/-}$, and *prmt8*$^{+/+}$; Fig. 2, G to I). Given that PLDs levels were unchanged, why was the level of PC increased in the cerebellum of *prmt8*$^{-/-}$ mice in which the dendritic trees of Purkinje cells were diminished? PLD1 negatively regulates the formation of dendritic branches in neurons (*33*), and PLD2 in particular is involved in axon outgrowth (*34*). To examine whether PLD activity is regulated by binding to PRMT8, we carried out coimmunoprecipitation experiments. However, the results suggested that PRMT8 did not interact with mammalian PLDs such as PLD1, PLD2, and the mitochondrial cardiolipin lipase MitoPLD (fig. S3). Therefore, another enzyme(s) may be required for PC hydrolysis in the context of dendritic arborization.

Eukaryotic PLDs contain a conserved catalytic amino acid sequence, $HxK(x)_4D(x)_6GG/S$ (where x represents any amino acid) (*35*), which is referred to as the HKD motif (fig. S4A). We found that this motif was well conserved in human, mouse, and zebrafish PRMT8 (Fig. 3A and fig. S4B) but not in other mammalian PRMTs (fig. S4C).

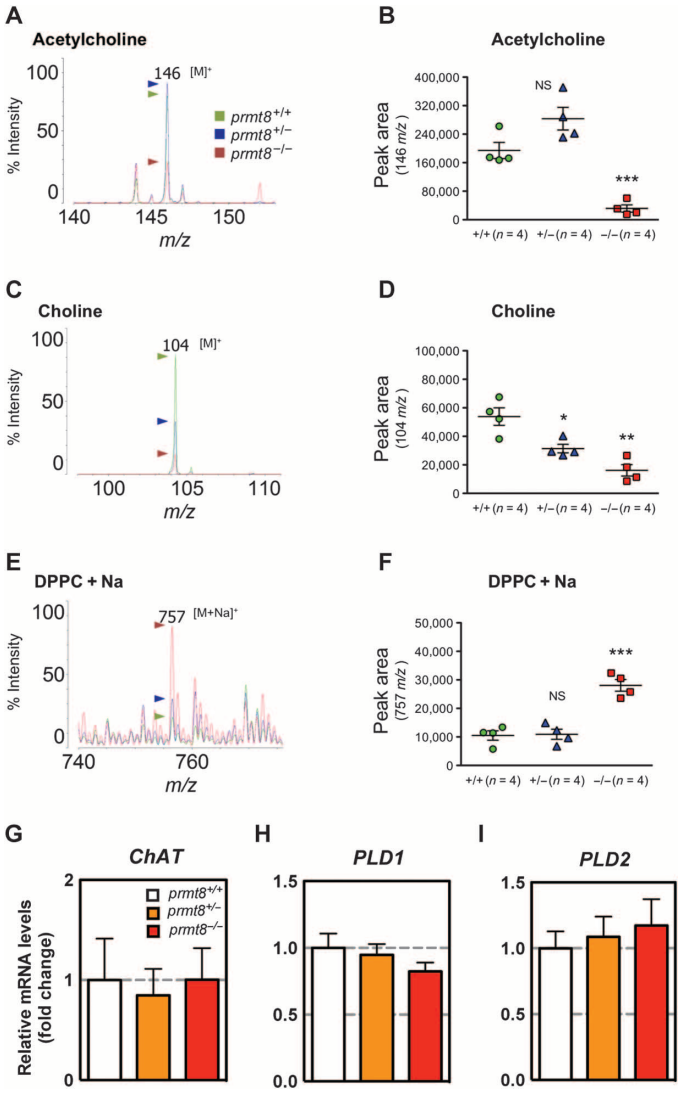

Fig. 2. Acetylcholine and choline are decreased, whereas PC levels are increased, in the cerebellum of *prmt8*$^{-/-}$ mice. (**A** to **F**) Specific detection of acetylcholine, choline, and PC by MALDI-QIT-TOF/MS. Positive-ion mode mass spectrum of acetylcholine (*m*/*z* 146 $[M]^+$) with α-cyano-4-hydroxycinnamic acid (CHCA), choline (*m*/*z* 104 $[M]^+$) with 9-aminoacridine hemihydrate (9-AA), or DPPC (*m*/*z* 757 $[M + Na]^+$) with 9-AA as matrix. The *m*/*z* ratios among the peaks are indicated. Among the three mouse genotypes (WT, heterozygous, and homozygous; $n = 4$ per genotype) examined, experimental ratios were determined by summing the ion peak areas. Data are shown as means ± SEM; $^*P < 0.05$, $^{**}P < 0.01$, $^{***}P < 0.0001$, or NS as compared to WT mice. (**G** to **I**) The mRNA expression of *ChAT*, *PLD1*, and *PLD2* was analyzed by qPCR. Results are shown as fold change of mRNA expression relative to the mean value of the WT sample. Data were obtained using the $\Delta\Delta C_t$ method normalized to the reference *GAPDH* mRNA (mean ± SEM, $n = 4$ per genotype; data were not significantly different).

Thus, to determine whether the conserved HKD motif in PRMT8 hydrolyzed PC to generate choline and PA, we used a green fluorescent protein (GFP)–tagged PA-binding domain (PABD) derived from residues 51 to 91 of yeast Spo20 as a sensor for PA. The fluorescent signal of GFP-PABD is usually observed in the nucleus but is translocated to the membrane when bound to PA (*36*, *37*). Specifically, we

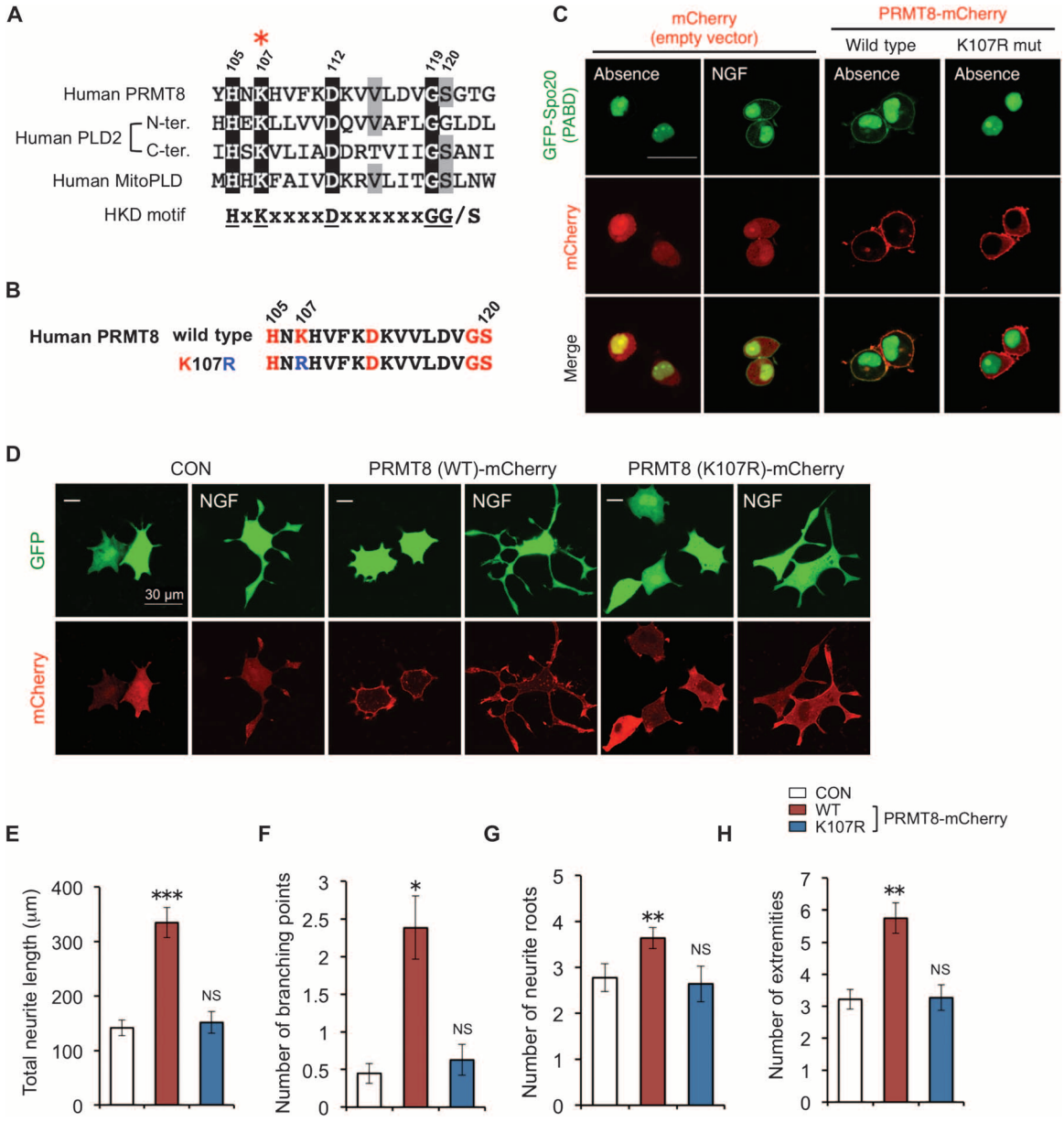

Fig. 3. Lysine 107–dependent PRMT8 induces neurite branching in NGF-stimulated PC12 cells. (**A**) Alignment of the amino acids in the HKD motifs from human PRMT8 and PLD2 and the mitochondrial PLD isoform MitoPLD. The amino acids that were mutated in the study are marked with a red asterisk. (**B**) Schematic representation of the K107R mutation generated in human PRMT8. (**C**) Translocation of GFP-PABD (Spo20$^{51–91}$), a PA sensor, to the plasma membrane upon PRMT8-mediated PA generation. PC12 cells were cotransfected with GFP-PABD and pmCherry vector (control), WT PRMT8-mCherry, or the PRMT8 K107R mutant. Controls were stimulated with or without NGF (100 ng ml^{-1}) for 5 min (left panel). Scale bar, 50 μm. Neurite development of NGF-differentiated PC12 cells. (**D**) PC12 cells were coexpressed with the pVenus vector and pmCherry vector (control), WT PRMT8-mCherry, or the PRMT8 K107R mutant, and stimulated with NGF (100 ng ml^{-1}) for 24 hours. Scale bars, 30 μm. (**E** to **H**) Cells bearing neurites that were twofold longer than their cell body lengths were scored in terms of (E) total neurite length, (F) the number of branching points per cell, (G) the number of neurite roots, and (H) the number of extremities. Results are shown as mean ± SEM of five independent experiments with at least 50 cells scored in each experiment; *P < 0.05, **P < 0.01, ***P < 0.0001, or NS as compared to the control (CON).

transfected PC12 cells with GFP-PABD and wild-type PRMT8 or with a PRMT8 point mutant (K107R) in which lysine 107 within the HKD sequences was replaced by arginine (Fig. 3B); the latter mutant was modeled after a lipase-inactive PLD that carried a lysine-to-arginine mutation of the lysine residue in the HKD motif (*38*). When wild-type human PRMT8-mCherry, but not the K107R mutant, was coexpressed with the GFP-PABD, it was partially translocated to the plasma membrane in PC12 cells (Fig. 3C). These results indicate that PRMT8 is involved in the production of PA at the plasma membrane in a lysine 107–dependent manner.

PA and its second messengers, such as diacylglycerol and lyso-PA, are involved in multiple biological functions including intracellular

signal transduction, lipid metabolism, and modulation of membrane structure (*39*). In addition, PA from PC hydrolysis promotes negative membrane curvature (*8*), which is essential for axon and dendrite morphogenesis (*40*). PC12 cells, which readily project neurites when stimulated with nerve growth factor (NGF), represent a convenient model of neuronal cell signaling (*41*). Moreover, PLD2-derived PA plays an important role in neurite outgrowth (*8*). To examine whether PRMT8 promotes neurite development in NGF-stimulated PC12 cells, we transfected these cells with either wild-type human PRMT8-mCherry or the PRMT8 K107R mutant and examined the cells for morphological changes (Fig. 3, D to H). We observed a marked increase in total neurite length and branch density in cells expressing wild-type PRMT8-mCherry as compared to cells transfected with the control mCherry vector. However, we saw little change in outgrowth or branch density in cells transfected with the PRMT8 K107R mutant even after NGF treatment. These data suggest that PRMT8 enhances neurite branching in NGF-stimulated PC12 cells and that this activity requires lysine 107.

All known classical PLDs have been shown to encode two copies of the HKD motif at the N and C termini, and a juxtaposed dimer-like structure of the two HKD motifs is required for the hydrolytic activity (*35*). On the other hand, MitoPLD, a member of the PLD family, encodes a single half-catalytic site and requires dimerization to function (*42*). Because a previous study demonstrated that PRMT8 is able to form homodimer (*10*), we tested whether wild-type PRMT8 or the K107R or methyltransferase-inactive G121A mutant interacts with itself using coimmunoprecipitation experiments. As shown in fig. S5, wild-type PRMT8-Flag was associated with wild-type PRMT8-HA,

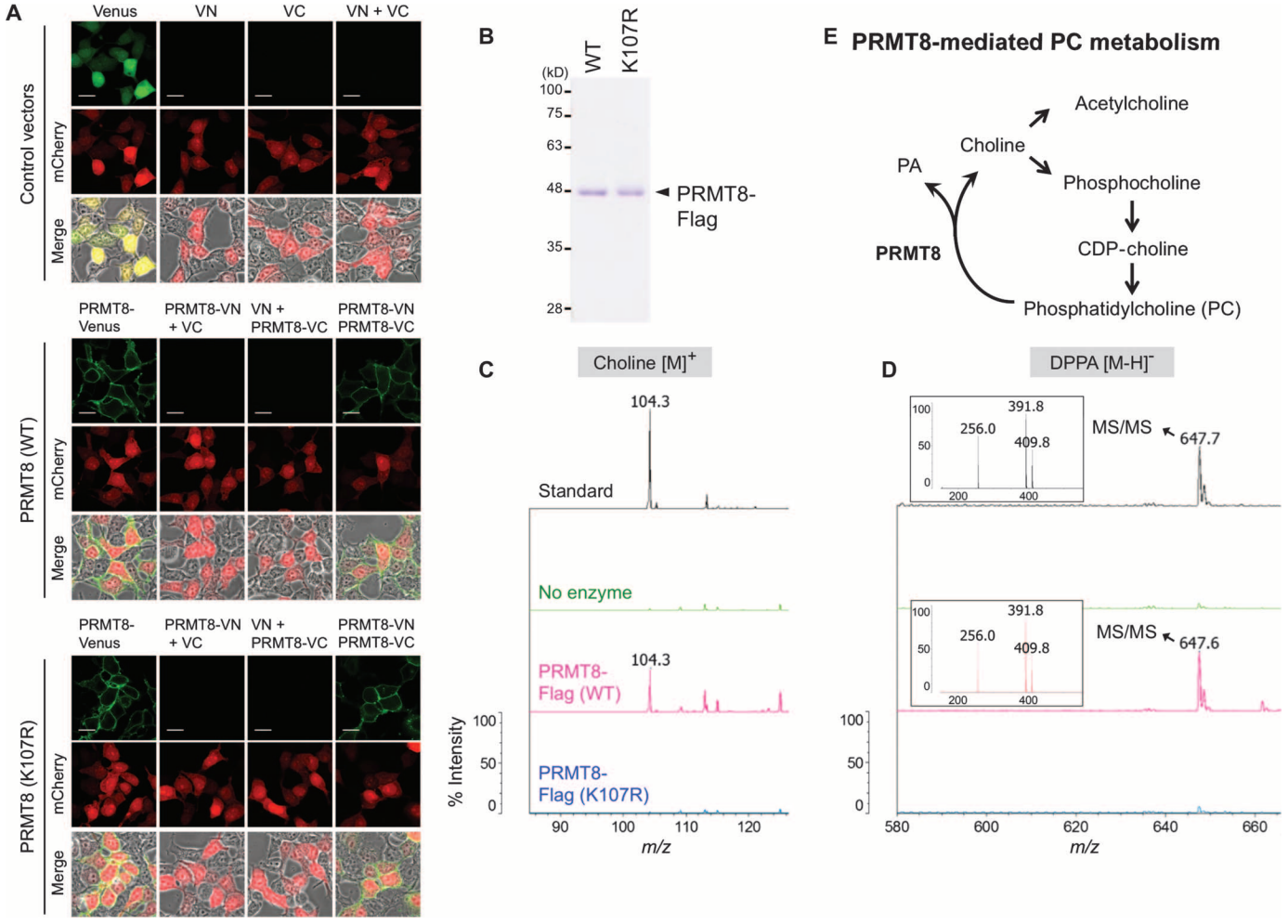

Fig. 4. PRMT8 is an HKD motif–dependent phospholipase. (**A**) BiFC experiments indicate dimerization of WT PRMT8 and the PRMT8 K107R mutant at the plasma membrane of HEK293T cells. All cells were cotransfected with BiFC pair vectors and mCherry vector as a transfection control. Scale bars, 20 μm. (**B**) Purified WT PRMT8 and the catalytically inactive PRMT8 K107R mutant were produced through baculoviral expression followed by Flag tag purification; proteins were visualized by Coomassie blue staining. (**C** and **D**) MS analysis of the reaction products generated by incubation of DPPC with either WT PRMT8-Flag or PRMT8 K107R mutant proteins. (C) Positive ion mode; (D) negative ion mode. Upper panels: Standard choline or DPPA with buffers but no enzyme. Middle panels: DPPC substrate with buffers but no enzyme. Bottom panels: DPPC substrate incubated with either WT PRMT8-Flag or PRMT8 K107R mutant proteins, resulting in the conversion of a portion of DPPC to the expected hydrolyzed products. Insets display the MS^2 spectra of the following DPPA peaks at *m/z* 647.6: palmitic acid, *m/z* 256.0 $[M - H]^-$; 16:0 lyso-PA, *m/z* 391.9 $[M - H_2O]^-$; 16:0 lyso-PA, *m/z* 409.8 $[M - H]^-$. (**E**) Proposed working model for PRMT8-mediated PC metabolism.

and the latter two mutants were biochemically homodimerized. Because PRMT8 encodes a single HKD motif, we considered that PRMT8 could be homodimerized to have the two motifs at the plasma membrane, and we analyzed the dimer formation by means of the bimolecular fluorescence complementation (BiFC) assay, using a Venus molecule that is split into N-terminal (VN) and C-terminal (VC) nonfluorescent portions (*43*). To detect the homodimerization of wild-type PRMT8 or the K107R mutant and identify their localization in cells, we generated fusion constructs, PRMT8-VN and PRMT8-VC, and cotransfected them into human embryonic kidney (HEK) 293T cells. Venus fluorescence was clearly yielded in the plasma membrane when cotransfected with wild-type PRMT8-VN and PRMT8-VC or with K107R mutant PRMT8-VN and PRMT8-VC (Fig. 4A). Thus, this result indicated that in the plasma membrane, the homodimeric form of PRMT8 could have the two copies of the HKD motif.

We previously reported a MALDI-QIT-TOF/MS method that directly detects DPPC-derived choline and dipalmitoylphosphatidic acid (DPPA) catalyzed by PLD (*44*). Because DPPC was significantly increased in the cerebellum of *prmt8*$^{-/-}$ mice, we investigated whether PRMT8, but not the PRMT8 K107R mutant, directly hydrolyzed DPPC to produce choline and DPPA. DPPC was incubated with purified wild-type human PRMT8-Flag or the PRMT8 K107R mutant (Fig. 4B), and choline at *m*/*z* 104.3 $[M]^+$ and DPPA at *m*/*z* 647.6 $[M - H]^-$ production were assessed by MS (fig. S6A). Figure 4 (C and D) shows that choline and DPPA were generated from DPPC by wild-type PRMT8, but not by the PRMT8 K107R mutant. Mouse and zebrafish PRMT8 also catalyzed the hydrolysis of DPPC to choline and DPPA (fig. S6, B to D). In addition, we also assessed the PC hydrolysis activity of PRMT8 using the headgroup-release assay with [choline-methyl-^{3}H]DPPC ([^{3}H]DPPC) as a substrate (*44*, *45*). As expected, wild-type PRMT8, but not the K107R mutant, generated [^{3}H]choline as a water-soluble product (fig. S7). These results clearly show that PRMT8 is an HKD motif–dependent PC-phospholipase in vitro.

PC metabolism plays an important role in at least two biological functions in neurons. First, PC-hydrolyzed choline is converted to acetylcholine as a neurotransmitter, regulating animal behaviors. In addition, PA is involved in morphological changes by altered composition of phospholipids on the plasma membrane. In these processes, it is well understood that PLD1 inhibits dendritic branching (*33*) and PLD2 promotes axonal outgrowth (*34*). Although PC metabolism in Purkinje cells is required for dendritic arbor formation, the type of enzymes involved remains unclear. Here, we propose that PRMT8 plays a pivotal role in phospholipid metabolism by modulating PC levels (Fig. 4E) and regulates brain function through maintenance of dendritic arborization in Purkinje cells. The PRMT8 K107R mutant was also able to catalyze arginine methylation (fig. S8C). By contrast, as shown in fig. S8 (D and E), choline and PA were generated from DPPC by the methyltransferase-inactive G121A mutant. A recent report has shown that serine 120 of PRMT8 is required for the protein arginine methyltransferase activity (*16*), which is completely overlapped with the HKD motif (fig. S8A). We also identified that the serine 120 to alanine (S120A) mutant of PRMT8 does not catalyze both arginine methylation and PC hydrolysis (fig. S9). Because PRMT8 has dual catalytic activities, further insights into PRMT8-mediated PC metabolism will improve our understanding of how the neuronal system functions and might help to identify the underlying causes of some neurological and developmental disorders.

MATERIALS AND METHODS

Animals

Animal experiments were carried out in a humane manner with the approval of the Institutional Animal Experiment Committee of the University of Tsukuba (Tsukuba, Japan). Experiments were performed in accordance with the Regulation of Animal Experiments of the University of Tsukuba and the Fundamental Guidelines for Proper Conduct of Animal Experiments and Related Activities in Academic Research Institutions under the jurisdiction of the Ministry of Education, Culture, Sports, Science, and Technology of Japan. The mouse line Prmt8$^{tm1a(EUCOMM)Wtsi}$ allele was generated by blastocyst injection of the JM8.F6 embryonic stem cell clone EPD0105_1_A03 produced by the European Conditional Mouse Mutagenesis Program and Knockout Mouse Project (EUCOMM/KOMP) and Sanger Mouse Genetics Project (www.mousephenotype.org/martsearch_ikmc_project/martsearch/project/34398; www.sanger.ac.uk/mouseportal/search?query=prmt8). The targeting construct contains four and six exons of *prmt8* and the PGK-neo cassette (Neo) flanked by two LoxP sites and the Neo flanked by FRT sites. Neo was removed by crossing with mice expressing FLPe under the control of the human β-actin promoter. Exon 5 of *prmt8* was deleted by mating *prmt8*$^{flox/+}$ mice with Ayu1-Cre mice, which ubiquitously express Cre recombinase. For genotyping of PRMT8 knockout mice, the tail genome was extracted with KAPA Express Extract, and multiplex allele-specific PCR was carried out with KAPA2G Robust HotStart ReadyMix with dye (Kapa Biosystems) according to the manufacturer's protocol using the following PCR primers: forward (P1), 5′-CCTGGCACTTTGAGGTGTTG-3′, and reverse (P2), 5′-TCCAGGATACACCACGTCCT-3′, which generated a 504-bp product for the *prmt8* wild-type allele; and reverse (P3), 5′-TCGTGGTATCGTTATGCGCC-3′, which generated a 252-bp product for the PRMT8 knockout allele.

Quantitative real-time PCR analysis

Total RNA was extracted from frozen cerebellum tissues using ISOGEN (NIPPON GENE Co.) and was quantified by NanoDrop (NanoDrop 2000, Thermo Scientific). All total RNA samples required A_{260}/A_{280} (absorbance at 260 and 280 nm) ratios of 1.98 to 2.00 for inclusion. Complementary DNA (cDNA) was synthesized from total RNA using ReverTra Ace (Toyobo). Gene expression was assessed using real-time PCR with SYBR Green PCR Master Mix and the Thermal Cycler Dice Real Time System (TAKARA BIO Inc.) under the following conditions: 1 cycle of 95°C for 30 s followed by 40 cycles of 95°C for 5 s, 60°C for 30 s, and then 95°C for 15 s and 60°C for 30 s, and finally 95°C for 15 s, carried out for dissociation analysis. Results were normalized to the housekeeping gene *GAPDH*, and the $\Delta\Delta C_t$ method was used for all real-time PCR analyses. Amplifications were done as technical duplicates. Primer sequences specific for the *PRMT8*, *ChAT*, *PLD1*, *PLD2*, and *GAPDH* genes can be found in table S1.

Immunofluorescence analysis

For immunofluorescence staining of brain sections, mouse brains were perfusion-fixed with 4% paraformaldehyde, cryoprotected in 30% sucrose solution, frozen in optimal cutting temperature compound (Tissue-Tek), and cut into 10-μm-thick sections. The frozen tissue sections were washed with phosphate-buffered saline (PBS; pH 7.4) and permeabilized in 5% bovine serum albumin/0.5% Triton X-100 in PBS for 30 min. After blocking endogenous biotin with an endogenous

avidin-biotin blocking kit (Nichirei) and M.O.M. blocking reagent (Vector Laboratories) according to the manufacturer's protocol, the sections were incubated overnight with anti-calbindin-D-28K antibody (1:2000; Sigma). Primary antibody binding was detected with M.O.M. biotinylated anti-mouse immunoglobulin G reagent (Vector Laboratories), subsequently stained with streptavidin-conjugated Cy3 (Vector Laboratories). For nuclear staining, Hoechst 33258 (Wako) was used. Fluorescence was visualized using a confocal laser scanning microscope (FluoView FV10i, Olympus).

Behavioral testing

Mice were group-housed (three to five per cage) with controlled temperature (24° ± 1°C, humidity 50 ± 5%) under a 12:12-hour light-dark cycle (lights on at 7:00 a.m., 7:00 p.m.) and had access to food and water available ad libitum. For the limb-clasping test, mice were suspended by their tails and recorded for 60 s to measure limb-clasping behavior. For the open-field test of locomotor function using the modified-SHIRPA protocol, mice were placed in a white circular arena (55 × 33 × 18 cm) surrounded by a visually uniform environment, in which the bottom is a white plate composed of 11 × 11–cm square grids. Locomotor activity was recorded as the number of squares each mouse visited by all four feet during the 30-s recording time in the arena. The arena was cleaned with 70% ethanol after each test.

Cerebellum tissue lysate

Mouse cerebellum tissue was lysed using a bath-type sonicator (Cosmobio, Bioruptor UCD-250) in PBS buffer. Tissue and cell debris were removed by centrifugation at 13,200 rpm at 4°C for 10 min. After centrifugation, supernatant was separated into hydrophobic and hydrophilic phases using ice-cold chloroform and methanol (2:1, v/v) according to the method of Bligh and Dyer (*46*). These phases were dried by centrifugation under vacuum at 45°C for 4 hours.

MALDI-QIT-TOF/MS

All chemicals were of the highest purity obtainable. Analytical standards of choline chloride and DPPA were obtained from Sigma-Aldrich and Wako Pure Chemical, respectively. 2,5-Dihydroxybenzoic acid (DHBA; Shimadzu), CHCA (Shimadzu), or 9-AA (Acros Organics) matrix was dissolved in 90% methanol. Matrix solution (0.5 μl) and 0.5 μl of reaction samples were deposited on a MALDI plate and left to dry at room temperature to prepare sample spots. Calibration was performed using the standard reagents of DHBA matrix (*m*/*z* 155.0 $[M + H]^+$; Shimadzu) and bradykinin fragment 1–7 (*m*/*z* 757.4 $[M + H]^+$; Sigma). MS experiments with MALDI-QIT-TOF/MS^n ($n = 1, 2$) were performed using a MALDI-QIT-TOF mass spectrometer (Shimadzu-Biotech) equipped with a nitrogen laser (337 nm). Each profile in MS and MS/MS mode was the result of 400 single laser shots (sum of 2 × 200) directed onto the selected sample preparation, which were accumulated to give the final mass spectrum or the collision-induced dissociation spectrum.

Construction of plasmid

The Bam HI/Not I restriction sites included in the PCR primers were used to introduce the amplified full-length mCherry (amino acids 1 to 237) cDNA into a Bam HI/Not I–restricted pEGFP-N1 expression vector (Clontech). Human PRMT8 was amplified by PCR with Human Fetal Brain Matchmaker cDNA Library (Clontech) as a template. Human PRMT8 K107R mutant was generated by site-directed mutagenesis. These cDNAs were ligated into pmCherry vectors at Eco RI/Sal I sites. The Spo20 PABD was amplified by PCR from *Saccharomyces cerevisiae* genomic DNA as a template (provided by K. Irie, University of Tsukuba, Japan), using the following PCR primers: forward, 5′-CCGGAATTCCATGGACAATTGTTCAGGAAG-3′, and reverse, 5′-GGCGTCGACCTAACTAGTCTTAGTGGCGTC-3′. cDNA was ligated into a pEGFP-C1 expression vector (Clontech) at Eco RI/Sal I restriction sites.

Cell culture, transfection, and differentiation assay

Rat pheochromocytoma PC12 cells were maintained in Dulbecco's modified Eagle's medium (Gibco) and Ham's F-12 (Wako) containing 5% (v/v) fetal bovine serum (FBS) (Cell Culture Technology), 5% horse serum (Gibco), and 1% antibiotic-antimycotic (Gibco) in a 5% CO_2 humidified incubator at 37°C. Cells were seeded on a dish (35 mm, ibidi) that had been coated with poly L-lysine at a density of 5×10^3 per dish and were transfected with Lipofectamine LTX (Invitrogen) according to the manufacturer's protocol. For the differentiation assay, 24 hours after transfection, the cells were cultured with NGF, which was added at a final concentration of 100 ng ml^{-1} to the serum-free cell culture medium, for 24 hours. The cells were fixed with 3.7% formaldehyde (Wako). Fluorescence images were acquired with identical imaging parameters using a confocal laser scanning microscope (FluoView FV10i, Olympus) and were batch-analyzed using HCA-Vision software (CRISO) through automated neuron body detection, neurite detection, and neurite analysis, with identical parameters. The areas of cell body and neurite outgrowth were visualized with Venus, and the nucleus was stained with Hoechst 33258 (Wako).

Protein preparation

Human wild-type PRMT8-Flag and K107R mutant were expressed in *Spodoptera frugiperda* (Sf9) insect cells. The gene encoding PRMT8 was cloned into a pFastBac vector. After infection with a baculovirus containing the PRMT8 gene, Sf9 cells were cultured at 27°C in Sf-900II SFM (Gibco) supplemented with 5% FBS for 48 hours. The cells were harvested and lysed in lysis buffer containing 50 mM tris-HCl (pH 7.5), 300 mM NaCl, 1% NP-40, 1 mM phenylmethylsulfonyl fluoride, and protease inhibitor cocktail (Nacalai Tesque). All proteins were purified using anti–Flag M2 agarose beads (Sigma) and were eluted from Flag-agarose beads in Flag peptide (Sigma). After the first affinity chromatography purification, the enzymes were further purified by HiTrap Q HP (GE Healthcare) anion exchange chromatography followed by Superose 6 10/300 GL (GE Healthcare) gel filtration chromatography.

BiFC assay

DNA fragments coding for the N-terminal (VN: 1 to 173 amino acids) and C-terminal (VC: 155 to 228 amino acids) moieties of Venus were generated by PCR and cloned into Not I/Kpn I restriction sites of a pEGFP-N1 vector (Clontech). Human wild-type PRMT8 and the K107R mutant were amplified by PCR using oligonucleotides incorporating Eco RI/Sal I restriction sites and omitting the stop codon. The amplified fragments were ligated into the corresponding sites of the pVenus-N1, pVenus-VN, or pVenus-VC expression vector. HEK293T cells were seeded in dishes and cultured for 24 hours before transfection. Cells were cotransfected with pmCherry as transfection control and full-length Venus, VN, VC, or BiFC pair VN and VC vectors. Cells images were captured using a confocal laser scanning microscope

(FluoView FV10i, Olympus) with an enhanced yellow fluorescent protein filter.

In vitro PC lipase assay for MS

For the in vitro lipase assay of PRMT8 using MALDI-QIT-TOF/MS, DPPC (Wako) was rehydrated in PBS buffer and was sonicated using a bath-type sonicator (Bioruptor UCD-250, Cosmo Bio). The final DPPC concentration was 50 nM. The purified proteins were incubated with DPPC in 1× PBS (pH 7.4) (Oxoid) at 37°C for 3 hours. The reaction was terminated by the addition of ice-cold chloroform/methanol (2:1, v/v). The aqueous and organic phases were extracted and dried by centrifugation under vacuum at 45°C for 4 hours.

Statistical analysis

Data are expressed as means ± SEM. Statistical analysis was performed using Prism 5 (GraphPad Software) or Microsoft Excel 2011 for Mac (Microsoft), and statistical significance was determined at the $^{*}P < 0.05$, $^{**}P < 0.01$, and $^{***}P < 0.0001$ levels using unpaired Student's t test and one-way (genotype) analysis of variance (ANOVA).

SUPPLEMENTARY MATERIALS

Supplementary material for this article is available at http://advances.sciencemag.org/cgi/content/full/1/11/e1500615/DC1

Materials and Methods

Fig. S1. Functional analysis of *prmt8* using zebrafish.

Fig. S2. Quantitative analysis of the gait abnormalities in the *prmt8*$^{-/-}$ mice.

Fig. S3. Interaction of PRMT8-Flag and mammalian PLDs.

Fig. S4. Organizations of the catalytic domains in PLD superfamily.

Fig. S5. Dimerization of PRMT8-Flag wild-type (WT) and K107R and G121A mutants.

Fig. S6. Measuring vertebrate PRMT8 paralog-derived products from PC by MALDI-QIT-TOF/MS.

Fig. S7. Measuring PRMT8-derived [^{3}H]choline from [^{3}H]DPPC using TLC method.

Fig. S8. Methyltransferase and PC phospholipase activities of PRMT8.

Fig. S9. Loss of catalytic activities of PRMT8 by replacing serine 120 to alanine.

Table S1. Primers used for qPCR quantification of mRNA.

Movie S1. Behavior of mice in a novel environment.

References (*47*–*50*)

REFERENCES AND NOTES

1. M. Manto, J. M. Bower, A. B. Conforto, J. M. Delgado-Garcia, S. N. F. da Guarda, M. Gerwig, C. Habas, N. Hagura, R. B. Ivry, P. Mariën, M. Molinari, E. Naito, D. A. Nowak, N. Oulad Ben Taib, D. Pelisson, C. D. Tesche, C. Tilikete, D. Timmann, Consensus paper: Roles of the cerebellum in motor control—The diversity of ideas on cerebellar involvement in movement. *Cerebellum* **11**, 457–487 (2012).
2. R. Apps, R. Hawkes, Cerebellar cortical organization: A one-map hypothesis. *Nat. Rev. Neurosci.* **10**, 670–681 (2009).
3. N. L. Cerminara, E. J. Lang, R. V. Sillitoe, R. Apps, Redefining the cerebellar cortex as an assembly of non-uniform Purkinje cell microcircuits. *Nat. Rev. Neurosci.* **16**, 79–93 (2015).
4. C. G. Dotti, G. A. Banker, Experimentally induced alteration in the polarity of developing neurons. *Nature* **330**, 254–256 (1987).
5. R. M. Gould, F. Connell, W. Spivack, Phospholipid metabolism in mouse sciatic nerve in vivo. *J. Neurochem.* **48**, 853–859 (1987).
6. L. Paoletti, C. Elena, P. Domizi, C. Banchio, Role of phosphatidylcholine during neuronal differentiation. *IUBMB Life* **63**, 714–720 (2011).
7. J. M. Carter, L. Demizieux, R. B. Campenot, D. E. Vance, J. E. Vance, Phosphatidylcholine biosynthesis via CTP:phosphocholine cytidylyltransferase 2 facilitates neurite outgrowth and branching. *J. Biol. Chem.* **283**, 202–212 (2008).
8. Y. Kanaho, Y. Funakoshi, H. Hasegawa, Phospholipase D signalling and its involvement in neurite outgrowth. *Biochim. Biophys. Acta* **1791**, 898–904 (2009).
9. J. E. Vance, E. P. De Chaves, R. B. Campenot, D. E. Vance, Role of axons in membrane phospholipid synthesis in rat sympathetic neurons. *Neurobiol. Aging* **16**, 493–498 (1995).
10. J. Lee, J. Sayegh, J. Daniel, S. Clarke, M. T. Bedford, PRMT8, a new membrane-bound tissue-specific member of the protein arginine methyltransferase family. *J. Biol. Chem.* **280**, 32890–32896 (2005).
11. J.-D. Kim, K. Kako, M. Kakiuchi, G. G. Park, A. Fukamizu, EWS is a substrate of type I protein arginine methyltransferase, PRMT8. *Int. J. Mol. Med.* **22**, 309–315 (2008).
12. S. Pahlich, R. P. Zakaryan, H. Gehring, Identification of proteins interacting with protein arginine methyltransferase 8: The Ewing sarcoma (EWS) protein binds independent of its methylation state. *Proteins* **72**, 1125–1137 (2008).
13. J. Sayegh, K. Webb, D. Cheng, M. T. Bedford, S. G. Clarke, Regulation of protein arginine methyltransferase 8 (PRMT8) activity by its N-terminal domain. *J. Biol. Chem.* **282**, 36444–36453 (2007).
14. M. B. C. Dillon, H. L. Rust, P. R. Thompson, K. A. Mowen, Automethylation of protein arginine methyltransferase 8 (PRMT8) regulates activity by impeding *S*-adenosylmethionine sensitivity. *J. Biol. Chem.* **288**, 27872–27880 (2013).
15. Z. Simandi, E. Czipa, A. Horvath, A. Koszeghy, C. Bordas, S. Póliska, I. Juhász, L. Imre, G. Szabó, B. Dezso, E. Barta, S. Sauer, K. Karolyi, I. Kovacs, G. Hutóczki, L. Bognár, Á. Klekner, P. Szucs, B. L. Bálint, L. Nagy, PRMT1 and PRMT8 regulate retinoic acid-dependent neuronal differentiation with implications to neuropathology. *Stem Cells* **33**, 726–741 (2015).
16. Y.-. Lin, Y.-J. Tsai, Y.-F. Liu, Y.-C. Cheng, C.-M. Hung, Y.-J. Lee, H. Pan, C. Li, The critical role of protein arginine methyltransferase *prmt8* in zebrafish embryonic and neural development is non-redundant with its paralogue *prmt1*. *PLOS One* **8**, e55221 (2013).
17. A. Kousaka, Y. Mori, Y. Koyama, T. Taneda, S. Miyata, M. Tohyama, The distribution and characterization of endogenous protein arginine N-methyltransferase 8 in mouse CNS. *Neuroscience* **163**, 1146–1157 (2009).
18. M. G. Rossmann, D. Moras, K. W. Olsen, Chemical and biological evolution of nucleotide-binding protein. *Nature* **250**, 194–199 (1974).
19. C. Sotelo, I. Dusart, Intrinsic versus extrinsic determinants during the development of Purkinje cell dendrites. *Neuroscience* **162**, 589–600 (2009).
20. K. J. Lee, J. G. Jung, T. Arii, K. Imoto, I. J. Rhyu, Morphological changes in dendritic spines of Purkinje cells associated with motor learning. *Neurobiol. Learn. Mem.* **88**, 445–450 (2007).
21. C. Belzung, G. Griebel, Measuring normal and pathological anxiety-like behaviour in mice: A review. *Behav. Brain Res.* **125**, 141–149 (2001).
22. H. Masuya, M. Inoue, Y. Wada, A. Shimizu, J. Nagano, A. Kawai, A. Inoue, T. Kagami, T. Hirayama, A. Yamaga, H. Kaneda, K. Kobayashi, O. Minowa, I. Miura, Y. Gondo, T. Noda, S. Wakana, T. Shiroishi, Implementation of the modified-SHIRPA protocol for screening of dominant phenotypes in a large-scale ENU mutagenesis program. *Mamm. Genome* **16**, 829–837 (2005).
23. M. Sarter, M. E. Hasselmo, J. P. Bruno, B. Givens, Unraveling the attentional functions of cortical cholinergic inputs: Interactions between signal-driven and cognitive modulation of signal detection. *Brain Res. Rev.* **48**, 98–111 (2005).
24. I. Klinkenberg, A. Sambeth, A. Blokland, Acetylcholine and attention. *Behav. Brain Res.* **221**, 430–442 (2011).
25. D. L. Zhang, C. X. Hu, D. H. Li, Y. D. Liu, Zebrafish locomotor capacity and brain acetylcholinesterase activity is altered by *Aphanizomenon flos-aquae* DC-1 aphantoxins. *Aquat. Toxicol.* **138–139**, 139–149 (2013).
26. O. Cohen, C. Erb, D. Ginzberg, Y. Pollak, S. Seidman, S. Shoham, R. Yirmiya, H. Soreq, Neuronal overexpression of "readthrough" acetylcholinesterase is associated with antisense-suppressible behavioral impairments. *Mol. Psychiatry* **7**, 874–885 (2002).
27. A. Mattsson, K. Pernold, S. O. Ögren, L. Olson, Loss of cortical acetylcholine enhances amphetamine-induced locomotor activity. *Neuroscience* **127**, 579–591 (2004).
28. K. Takase, Y. Sakimoto, F. Kimura, D. Mitsushima, Developmental trajectory of contextual learning and 24-h acetylcholine release in the hippocampus. *Sci. Rep.* **4**, 3738 (2014).
29. J. K. Blusztajn, M. Liscovitch, U. I. Richardson, Synthesis of acetylcholine from choline derived from phosphatidylcholine in a human neuronal cell line. *Proc. Natl. Acad. Sci. U.S.A.* **84**, 5474–5477 (1987).
30. D. Zhao, M. A. Frohman, J. K. Blusztajn, Generation of choline for acetylcholine synthesis by phospholipase D isoforms. *BMC Neurosci.* **2**, 16 (2001).
31. R. S. Jope, D. J. Jenden, Choline and phospholipid metabolism and the synthesis of acetylcholine in rat brain. *J. Neurosci. Res.* **4**, 69–82 (1979).
32. W. C. Colley, T.-C. Sung, R. Roll, J. Jenco, S. M. Hammond, Y. Altshuller, D. Bar-Sagi, A. J. Morris, M. A. Frohman, Phospholipase D2, a distinct phospholipase D isoform with novel regulatory properties that provokes cytoskeletal reorganization. *Curr. Biol.* **7**, 191–201 (1997).
33. Y.-B. Zhu, K. Kang, Y. Zhang, C. Qi, G. Li, D.-M. Yin, Y. Wang, PLD1 negatively regulates dendritic branching. *J. Neurosci.* **32**, 7960–7969 (2012).
34. H. Watanabe, T. Yokozeki, M. Yamazaki, H. Miyazaki, T. Sasaki, T. Maehama, K. Itoh, M. A. Frohman, Y. Kanaho, Essential role for phospholipase D2 activation downstream of ERK MAP kinase in nerve growth factor-stimulated neurite outgrowth from PC12 cells. *J. Biol. Chem.* **279**, 37870–37877 (2004).
35. A. J. Morris, J. Engebrecht, M. A. Frohman, Structure and regulation of phospholipase D. *Trends Pharmacol. Sci.* **17**, 182–185 (1996).
36. H. Nakanishi, P. de los Santos, A. M. Neiman, Positive and negative regulation of a SNARE protein by control of intracellular localization. *Mol. Biol. Cell* **15**, 1802–1815 (2004).
37. M. Zeniou-Meyer, N. Zabari, U. Ashery, S. Chasserot-Golaz, A.-M. Haeberlé, V. Demais, Y. Bailly, I. Gottfried, H. Nakanishi, A. M. Neiman, G. Du, M. A. Frohman, M.-F. Bader, N. Vitale,

Phospholipase D1 production of phosphatidic acid at the plasma membrane promotes exocytosis of large dense-core granules at a late stage. *J. Biol. Chem.* **282**, 21746–21757 (2007).
38. T.-C. Sung, R. L. Roper, Y. Zhang, S. A. Rudge, R. Temel, S. M. Hammond, A. J. Morris, B. Moss, J. Engebrecht, M. A. Frohman, Mutagenesis of phospholipase D defines a superfamily including a *trans*-Golgi viral protein required for poxvirus pathogenicity. *EMBO J.* **16**, 4519–4530 (1997).
39. G. van Meer, D. R. Voelker, G. W. Feigenson, Membrane lipids: Where they are and how they behave. *Nat. Rev. Mol. Cell Biol.* **9**, 112–124 (2008).
40. H. T. McMahon, J. L. Gallop, Membrane curvature and mechanisms of dynamic cell membrane remodelling. *Nature* **438**, 590–596 (2005).
41. D. G. Drubin, S. C. Feinstein, E. M. Shooter, M. W. Kirschner, Nerve growth factor-induced neurite outgrowth in PC12 cells involves the coordinate induction of microtubule assembly and assembly-promoting factors. *J. Cell Biol.* **101**, 1799–1807 (1985).
42. S.-Y. Choi, P. Huang, G. M. Jenkins, D. C. Chan, J. Schiller, M. A. Frohman, A common lipid links Mfn-mediated mitochondrial fusion and SNARE-regulated exocytosis. *Nat. Cell Biol.* **8**, 1255–1262 (2006).
43. T. K. Kerppola, Design and implementation of bimolecular fluorescence complementation (BiFC) assays for the visualization of protein interactions in living cells. *Nat. Protoc.* **1**, 1278–1286 (2006).
44. K.-. Park, J.-. Kim, Y. Nagashima, K. Kako, H. Daitoku, M. Matsui, G. G. Park, A. Fukamizu, Detection of choline and phosphatidic acid (PA) catalyzed by phospholipase D (PLD) using MALDI-QIT-TOF/MS with 9-aminoacridine matrix. *Biosci. Biotechnol. Biochem.* **78**, 981–988 (2014).
45. A. J. Morris, M. A. Frohman, J. Engebrecht, Measurement of phospholipase D activity. *Anal. Biochem.* **252**, 1–9 (1997).
46. E. G. Bligh, W. J. Dyer, A rapid method of total lipid extraction and purification. *Can. J. Biochem. Physiol.* **37**, 911–917 (1959).
47. S. Kani, Y.-K. Bae, T. Shimizu, K. Tanabe, C. Satou, M. J. Parsons, E. Scott, S.-. Higashijima, M. Hibi, Proneural gene-linked neurogenesis in zebrafish cerebellum. *Dev. Boil.* **343**, 1–17 (2010).
48. V. M. Bedell, Y. Wang, J. M. Campbell, T. L. Poshusta, C. G. Starker, R. G. Krug II, W. F. Tan, S. G. Penheiter, A. C. Ma, A. Y. H. Leung, S. C. Fahrenkrug, D. F. Carlson, D. F. Voytas, K. J. Clark, J. J. Essner, S. C. Ekker, In vivo genome editing using a high-efficiency TALEN system. *Nature* **491**, 114–118 (2012).
49. Y.-K. Bae, S. Kani, T. Shimizu, K. Tanabe, H. Nojima, Y. Kimura, S.-. Higashijima, M. Hibi, Anatomy of zebrafish cerebellum and screen for mutations affecting its development. *Dev. Biol.* **330**, 406–426 (2009).
50. I. Lopez, R. S. Arnold, J. D. Lambeth, Cloning and initial characterization of a human phospholipase D2 (hPLD2). ADP-ribosylation factor regulates hPLD2. *J. Biol. Chem.* **273**, 12846–12852 (1998).

Acknowledgments: We thank W. Jin, M. Hashimoto, T. Shirakawa, M. Matsui, M. Kakiuchi, and M. Koike for their technical support; A. Miyawaki (RIKEN, Japan) for providing the plasmid for Venus; and the Open Innovation Core (OIC) project (J.-D.K. and J.H.; a member of OIC) of Life Science Center, Tsukuba Advanced Research Alliance (TARA), University of Tsukuba, Japan. We also thank the members of the Fukamizu laboratory for the helpful discussions. **Funding:** This work was supported, in part, by a Grant-in-Aid for Scientific Research (A) (to A.F.) (22248040), a Grant-in-Aid for Scientific Research (A) (to A.F.) (25252062), and a MEXT Grant-in-Aid Project (Scientific Research on Innovative Areas) (to A.F.) (23116001). **Author contributions:** J.-D.K. and A.F. planned and designed the experiments and analyzed the data. J.-D.K., K.-E.P., and K.K. performed the in vitro PC lipase assay with MALDI-QIT-TOF/MS, Y. Kanaho helped with the analysis of phosphatidylcholine-lipase activity, and J.-D.K. and J.I. assisted with the mouse intervention studies. J.H. carried out and evaluated the immunofluorescence analysis, and K.N. and Y. Kasuya helped with the analysis of the immunofluorescence data. J.-D.K. performed the neurite assay using PC12 cells, and S.F. helped with the analysis of the assay results. S.K., M.T., M.H., and M.K. designed and performed knockdown studies in zebrafish. H.F. and N.M. generated and analyzed the knockout zebrafish line. J.-D.K. and A.F. wrote the manuscript. All authors discussed and approved the manuscript. **Competing interests:** The authors declare that they have no competing interests. **Data and materials availability:** All data needed to evaluate the conclusions in the paper are present in the paper and/or the Supplementary Materials. Additional data related to this paper may be requested from A.F. (akif@tara.tsukuba.ac.jp).

Submitted 15 May 2015
Accepted 21 October 2015
Published 4 December 2015
10.1126/sciadv.1500615

Citation: J.-D. Kim, K.-E. Park, J. Ishida, K. Kako, J. Hamada, S. Kani, M. Takeuchi, K. Namiki, H. Fukui, S. Fukuhara, M. Hibi, M. Kobayashi, Y. Kanaho, Y. Kasuya, N. Mochizuki, A. Fukamizu, PRMT8 as a phospholipase regulates Purkinje cell dendritic arborization and motor coordination. *Sci. Adv.* **1**, e1500615 (2015).